IIETA International Information and Engineering Technology Association
Advancing the World of Information and Engineering

Mathematical Modelling of Engineering Problems
Vol. 9, No. 4, August, 2022, pp. 1095-1106
Journal homepage: http://iieta.org/journals/mmep

# Punching Shear Behavior of Flat Slab Strengthen with Y-Type Perfobond Shear

Daniah Abdulnasser Abdair*, Abdulnasser M. Abbas, Haleem K. Hussain

Department of Civil Engineering, College of Engineering, University of Basrah, Basrah 61004, Iraq

Corresponding Author Email: dnyahabdalnasser@gmail.com

https://doi.org/10.18280/mmep.090428

**Received:** 7 April 2022
**Accepted:** 1 August 2022

***Keywords:***
*flat slab, punching shear, steel fiber, shear reinforcement, Y-type perfobond, ABAQUS, finite element analysis*

**ABSTRACT**

This study demonstrates the behavior of a flat slab experimentally and numerically with two different types of shear reinforcements. Ten slabs were cast and tested in the experimental part. The samples were divided into two groups; the first consists of steel fiber, and the second has no steel fiber. Two control samples were considered with only flexural reinforcement, while the other eight samples had two types of shear reinforcement; the first was rebar to form a Y-shape, while the other was a steel plate formed as a Y-type perfobond. Shear reinforcement is provided by employing radial and parallel shear reinforcement. The tested samples in the experimental part have been simulated numerically using the Abaqus/CAE program. As a result of the laboratory examination, it was determined that the addition of steel fibers increased the ultimate load by (7.4% to 20.58%) for models with steel fibers compared to models without steel fibers. It was determined that the presence of steel plates in the models increased their capacity by 2.4% for ultimate load and by (6% to 50%) for deflection compared to ultimate load and deflection in models with steel bars. In Abaqus, the models with steel fibers were found to be 12.7%-26.6% stronger than those without them.

## 1. INTRODUCTION

The most common structural system is a flat slab. There is no projection of beams, drop panels, or capitals on the flat slabs of concrete, which transfer the load directly to the columns [1]. For flat slabs and flat plates supported directly by columns, the shear may be the critical factor in design. In almost all tests of such structures, failures have been due to shear or perhaps shear and torsion. These conditions are particularly significant around exterior columns [2]. The ACI code [3] specifies that critical sections in a two-way slab without shear reinforcement shall be located at least d/2 away from the edges and corners of columns. When shear reinforcement is used on two-way members, the critical section is positioned d/2 beyond the discontinuation of shear reinforcement. Perimeters located 2d from the column edge are considered in Eurocode 2 [4]. According to this code, the control perimeter consists of a rounded shape located at a distance (k.d) from the shear reinforcement tip (k=1.5). Generally, steel fiber acts as a crack arrestor, resisting the growth of cracks [5].

Many studies focused on the flail of the flat slab and its behavior under punching shear. In 1990, Hussein and Marzouk [6] used an experimental program to investigate flat slabs cast with (HSC). The results of the tests showed that HSC slabs that failed under punching shear had fewer deformations than those that failed under flexure punching. The effect of reinforcement on the flexural and shear stress of flat slabs was studied by Rasha et al. [7] throughout the casting and testing of seven half-slabs with 1050*1050*100 mm. They conclude that all of the specimens failed due to brittle punching, and punching capacity increased by 23% when adding vertical shear reinforcement for a spacing of 100 mm and 36% for a spacing of 50 mm, and the punching shear capacity of a flat slab was enhanced by the flexural tensile reinforcement which is above the column. The punching shear capacity improved by 6% when the ratio of flexural reinforcement was increased to 20% from the control specimen. From a summary of the flat slab, the problem of punching shear and its reinforcement were studied by Saadoon et al. [8]. They concluded that with the use of swimmer bars, the capacity of the punching shear is likely to increase by 17% as compared with a flat slab that has punching reinforcement. Shear failure in the slab can occur as a result of struts crushing concrete and shear punching in the outside area of its reinforcement. To enhance punching resistance and solve durability issues, the FRPs might be considered a new sort of shear reinforcement. Jang and Kang [9] investigated the effect of flexural and shear reinforcement on the strength of punching shear slab–column connections. They used six slab–column specimens with varying flexural and shear reinforcements applied to gravity load tests. The slab–column attachment behaved differently according to the amount of shear and flexural reinforcements. According to the experimental results, the strength of punching in the specimens with and without reinforcement of shear was increased by flexural reinforcement in the slab–column attachment. Abbas et al. [10] numerically analyzed the non-linear behavior of flat slabs utilizing ABAQUS software. Two specimens were considered, one being a flat slab reinforced with ordinary steel reinforcement, while the slab-column connection in the second one has been improved with Z-shaped shear rebar. They found that the proposed model reasonably improved the flat slab. Von-Mises stresses, punching shear, and deformations are all considered in their analysis. The Z-shaped reinforcement increases the strength of punching shear by 11.1%, with a decrease in deflection of 77.3% when used. In the meantime,

the slab-column connection became less stressed, and the stress concentrations moved away from it. In 2022, Sine et al. [11] conducted a study about the improvement of flat slabs, such as adding ultra-high-performance fiber-reinforced cementitious composites (UHPFRC) to existing reinforced concrete (RC) flat slabs increases their durability and flexural capacity significantly. Talib and Al-Salim [12] investigated the punching shear reinforcement placement with "the Ultrahigh Performance Concrete" (UHPC) and determined its optimal use in the shear area. However, due to its high cost, it was not feasible to use it in the whole slab. In addition, it was conducted at two different depths. As compared with the reference sample of normal concrete with reinforced flexural steel only, the slab cast with UHPC in all thicknesses of the sample showed an increase in punching shear strength. Additionally, UHPC cast at half the slab thickness does not produce satisfactory results compared to casting at entire thickness.

Moreover, there are several studies about using fibers in the flat slab to improve shear strength, as conducted by Michels et al. [13], Ju et al. [14], Moreno et al. [15], Mohammed et al. [16] by investigating the behavior of bearing in flat slabs with steel fiber and concluding that it can be used to improve the shear strength. Zamri et al. [17] review the parameters used in several existing experimental types of research about the steel fiber performance in reinforced concrete to improve the strength of punching shear in the flat slab. The efficacy of steel fiber in resisting the punching shear was found to be affected by volume fractions of fiber, material preparation, and specimen size. In 2022, Zamri et al. [18] studied "steel fiber reinforced self-compacting concrete" (SFRSCC), which offers an efficient mechanism of reinforcement. A slab with SFRSCC had a punching shear resistance 16.1%-34.8% higher than a slab with self-compacting concrete.

In flat slabs, Y-type plates were not used before; they had only been used in composite structures by Kim et al. [19], who was the first to employ the perfobond rib as a Y-type shear connector (see Figure 1). They did a study to verify the efficiency of shear connectors by using rib as a Y-type perfobond in composite members. They conclude that the variance in final load is due to rib width, height, and the compressive strength of concrete. As a result, a more efficient and economical design for applying the Y-type perfobond to composite structures has been developed.

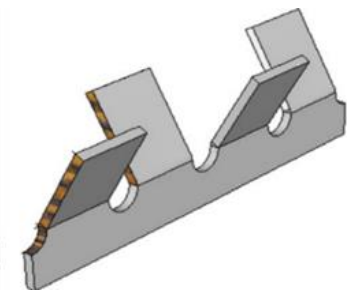

**Figure 1.** Y-shaped ribs [19]

This work aimed to study the shear behavior of the flat slab by testing its strength with different reinforcement forms (Y-type perfobond plate and Y-shape rebar), with flexural reinforcement, and different concrete types (with and without steel fiber) using two control specimens that had only flexural reinforcement, one with steel fiber, and the other having no steel fiber.

## 2. EXPERIMENTAL PROGRAM

### 2.1 Material

In the current study, the cement utilized to cast the specimens was Ordinary Portland, manufactured by an Iraqi factory (Falcon), which met the Iraqi Standard Specification No.5/2019 [20]. Coarse and fine aggregate from Jabal Sanam in Basrah were used in concrete mixes, and their properties conform to Iraqi Specifications No. 45/1984 [21]. The steel fiber used in this study was ends-hooked as in Figure 2 by the Bondrex company in Korea [22]. The technical properties of steel fiber are according to ASTM A820 [23]. Ukrainian steel rebar has been considered in this work. Rebar of diameter (Ø 12 mm) was employed as flexural reinforcement, while (Ø 10 mm) was employed for shear reinforcement. The shear reinforcement bar is formed to give a Y-type shape, as shown in Figure 3. All bars were tested to determine the required properties according to ASTM A615/A615M-04b [24]. Steel plates available in the local market with a 2 mm thickness were used. Steel plate specimens were tested to specify their properties.

The dimensions of steel plate specimens are shown in Figure 4. The plates' properties conform to ASTM A36/A 36M-05 [25]. The mix of concrete was designed according to (ACI 211.1-91) [26] to get compressive strength (30) MPa. Two concrete mixes were used in this test; the first was without steel fiber, and the second was with steel fiber. In the second mixture, the percentage of steel fibers used was 1% (ratio from steel's density equal to 7850 Kg/m3), as an approximate average of values adopted in several previous studies [13, 14, 27].

**Figure 2.** Steel fiber ends (Hooked)

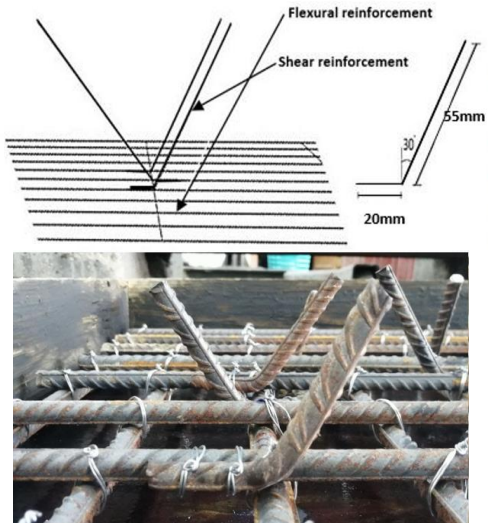


**Figure 3.** Y-type bar for shear reinforcement

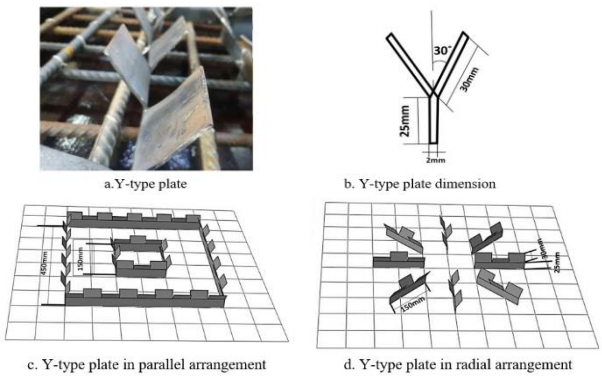


**Figure 4.** Detail of Y-type plate for shear reinforcement

### 2.2 Slabs details

The experimental work includes testing ten specimens, as shown in Table 1. The main objective of the experimental test is to study the effect of punching shear in concrete flat slabs with some variations like the type of shear reinforcement (bar as Y-type and plate as Y-type) and distribution of shear reinforcement (redial or parallel distribution, as shown in Figure 4c and d and with or without steel fiber, and also using control specimens without shear reinforcement. The samples had (800*800*100) mm dimensions, and the ratio of flexural reinforcement was (0.02). Shear reinforcements were designed to cover the shear critical area according to the ACI Code [3] and Eurocode 2-2004 [4] as described in section (1).

**Table 1.** Details of tested samples

| Item | Slab title | $f_c'$ MPA | Fiber | Dimension (mm x mm) | Flexural bar diameter (mm) | Shear plate thickness (mm) | Shear bar diameter (mm) |
|---|---|---|---|---|---|---|---|
| 1 | S1 | 30 | Without fiber | 800x800x100 | 12 | - | - |
| 2 | S1Pp* | 30 | | 800x800x100 | 12 | 2 | - |
| 3 | S1Rp** | 30 | | 800x800x100 | 12 | 2 | - |
| 4 | S1Pb | 30 | | 800x800x100 | 12 | - | 10 |
| 5 | S1Rb | 30 | | 800x800x100 | 12 | - | 10 |
| 6 | S2 | 30 | With fiber | 800x800x100 | 12 | - | - |
| 7 | S2Pp | 30 | | 800x800x100 | 12 | 2 | - |
| 8 | S2Rp | 30 | | 800x800x100 | 12 | 2 | - |
| 9 | S2Pb | 30 | | 800x800x100 | 12 | - | 10 |
| 10 | S2Rb | 30 | | 800x800x100 | 12 | - | 10 |

*S1Pp: Slab in group (1) with Parallel plate
**S1Rp: Slab in group (1) with Radial plate

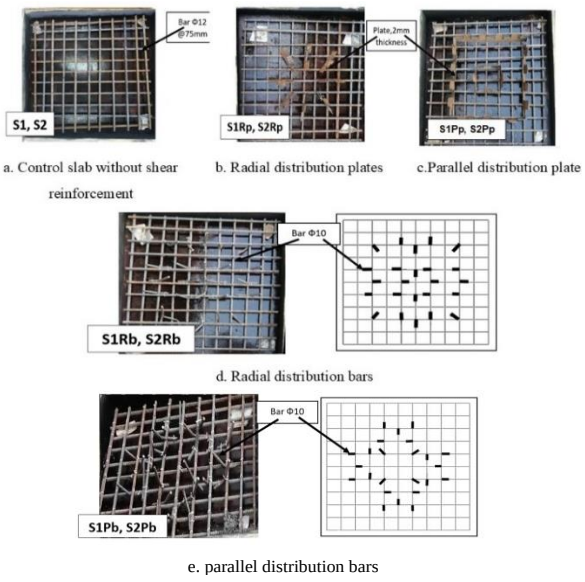


**Figure 5.** Variation in reinforcement in specimens

The specimens were divided into two group, the first group without steel fiber in concrete mix and the second with steel fiber in concrete mix. Two specimens were control specimens without shear reinforcement but with flexural reinforcement, one of them (S1) without steel fiber and another (S2) with steel fiber, as in Figure 5a. Four specimens (two in each group) with shear reinforcement made of the plates were formed to give a Y-type shape, two (S1Rp, S2Rp) as in Figure 5b were arranged radially, and two (S1Pp, S2Pp) arranged parallelly as in Figure 5c. Four slabs (two in each group) with shear reinforcement made of the bar (Ø 10) mm and a total length of 55 mm fixed on the top of the flexural reinforcement layer, two of these specimens (S1Rb, S2Rb) arranged in a radial distribution as in Figure 5d, and two (S1Pb, S2Pb) arranged in a parallel distribution as in Figure 5e.

### 2.3 Experimental test

Six cubes of (150 * 150 * 150) mm were tested at 28 days. The compressive strength was 38.9 MPA for normal concrete, while the strength was 40.65 for concrete with steel fiber. All tests were conducted in the material laboratory at the University of Bsarah, College of Engineering, Department of Civil Engineering. Test specimens were supported by a rigid steel frame, and the top surface of the frame's square steel plate was welded with four bars of 25 mm in diameter and 700 mm in length to provide simple support for a slab, as in Figures 6 and 7. The load was applied at (100 x 100) mm area, and the increase in load was (0.5-1) ton. To detect the deflection at any loading stage, the gage sensor is located as shown in Figure 8.

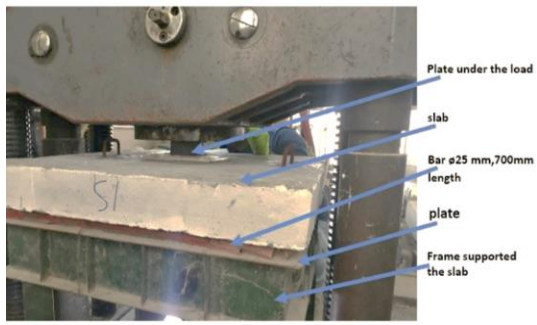


**Figure 6.** Supported system

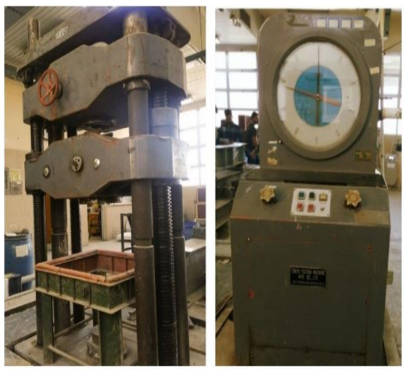

**Figure 7.** Slab test machine

**Figure 8.** Deflection gage sensor

**Table 2.** Ultimate load capacity and maximum deflection in group

| Specimens Item | Ultimate load KN | First cracking load | Increase in cracking load % | Increase in ultimate load % | Maximum deflection mm |
|---|---|---|---|---|---|
| S1 | 135 | 20 | - | - | 6.11 |
| S1Rp | 175 | 35 | 75% | 30% | 4.32 |
| S1Rb | 170 | 33 | 65% | 26% | 5.89 |
| S1Pp | 165 | 30 | 50% | 22% | 6.69 |
| S1Pb | 150 | 25 | 25% | 11% | 7.1 |
| S2 | 145 | 30 | - | - | 6.9 |
| S2RP | 185 | 60 | 100% | 28% | 9.03 |
| S2Rb | 180 | 50 | 67% | 24% | 9.8 |
| S2Pp | 210 | 45 | 50% | 45% | 8.81 |
| S2Pb | 205 | 40 | 33% | 41% | 10.1 |

### 2.4 Experimental result

The obtained results include the first crack load, failure load, and deflection, as shown in Table 2.

2.4.1 The slab behavior and cracking patterns

On the tensile face of all slabs, cracks develop from the center and expand outward. With the load increasing, the cracks extended, and new cracks developed. Different crack patterns were observed on the bottom surface of slabs according to the type and arrangement of shear reinforcement and concrete kind. Figure 9 presents general patterns of cracking after failure. It has been observed that no cracks can be seen on the compression face of slabs, except for those top surfaces under the loaded area. In experimental work, the first crack loads are elevated by (25%-100%), as compared to control slab crack loads, increasing the elastic range.

2.4.2 Punching shear behavior

The punching shear strength of slabs has been calculated using many different formulas. Under the ACI code [3], shear stress is expressed as a square - root function of concrete compressive strength, whereas in Eurocode 2 [4], it is calculated as a cubic-root function of concrete compressive strength. Based on Eurocode 2, the reinforcement ratio is considered, so the shear stress is 113 kN, while the ACI code provides a shear stress of 94.8 kN because this code disregards the effect of reinforcement ratios. Figure 9 shows the punching shear located at the intersection of 0.5 d of the column edge and 1.5 d of the reinforcement ends.

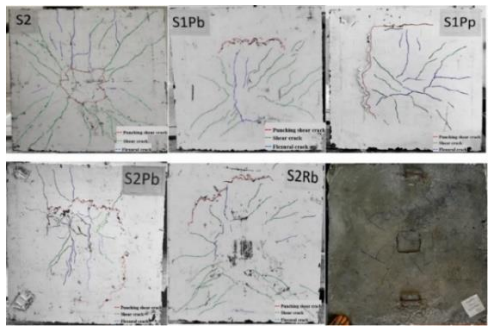


**Figure 9.** Crack in tension and compression face of slab for different reinforcement

2.4.3 Effect of steel fiber on ultimate load and first cracking load

Figures 10a and 10b depict a comparison between models with and without fiber for the influence of steel fiber on ultimate load and the first cracking load, respectively. In samples without shear reinforcement, steel fiber increased the ultimate load by 7% and delayed the cracking load by 50%. The maximum increase in ultimate load for the sample with shear reinforcement and steel fiber was 55% when compared with the sample without shear reinforcement and steel fiber (S1). The maximum percentage of the ultimate load increase caused by added fibers was 36.6% in the sample with shear reinforcement compared to the sample with shear reinforcement but without steel fibers. As found by Tayfun Uygunoğlu [28], the existence of the steel fibers that are used in concrete prevents crack propagation.

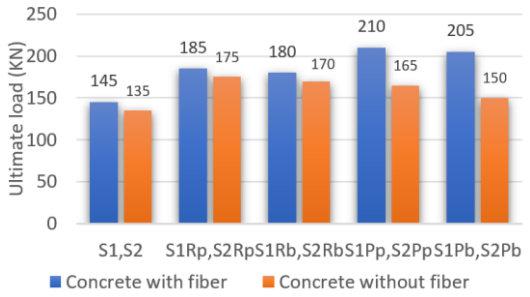


(a) The Effect of steel fibres on ultimate load

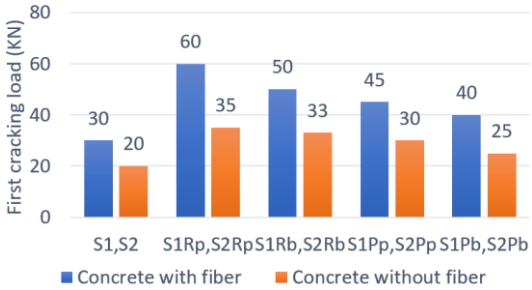


(b) The Effect of steel fibres on first cracking load

**Figure 10.** The effect of steel fiber

2.4.4 Effect of Plate shear reinforcement on ultimate load and first cracking load

Shear reinforcement with steel plates in radial and parallel distribution increased the slab's bearing capacity and first cracking load. In (S1Rp), for instance, the ultimate and cracking load are higher than the ultimate and cracking load of bar reinforcement in (S1Rb), as shown in Figure 11a and 11b. The increase in bearing capacity was represented by more ultimate and cracking load and less deflection in slabs with plates than in slabs with bars, by (2.4% and 10%) for ultimate and crack load and (6%-50%) for maximum deflection, due to the larger surface area of the plates, which at least will increasingly interact with the concrete mixture. Kim et al. proved this principle when comparing Y-type perfobond and studs in composite girders [19].

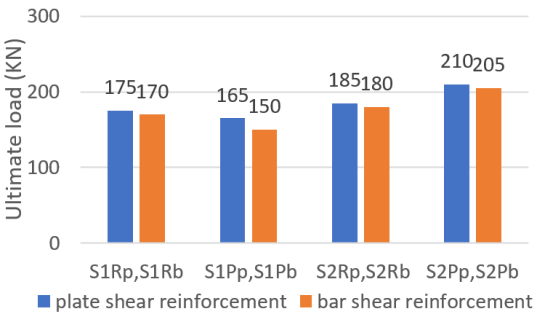


(a) The effect of a plate on ultimate load

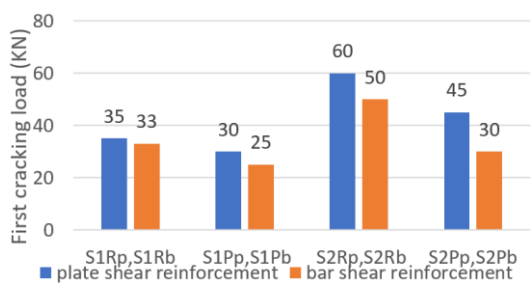


(b) The effect of a plate on First crack load

**Figure 11.** The effect of a plate shear reinforcement

2.4.5 The effect of reinforcement distribution On Ultimate and first crack load

Figures 12a and 12b show that in slabs without steel fiber, the radial distribution of shear reinforcement gives more capacity than the parallel distribution of shear reinforcement and the max percentage (6.2% and 32%) for the ultimate and cracking load respectively. While in a slab with steel fiber, the parallel distribution of shear reinforcement was the stronger about (13.8%-33.3%) for the ultimate and cracking load. The strong radial shear reinforcement distribution in slab without fiber was observed by Sheikh and Sissakis [29], and they attributed the reason to radially reinforced action, which offered less distance between reinforcements to prevent shear failures within the shear-reinforced zone. Figure 13 shows the difference in maximum distance between the bars in shear reinforcement.

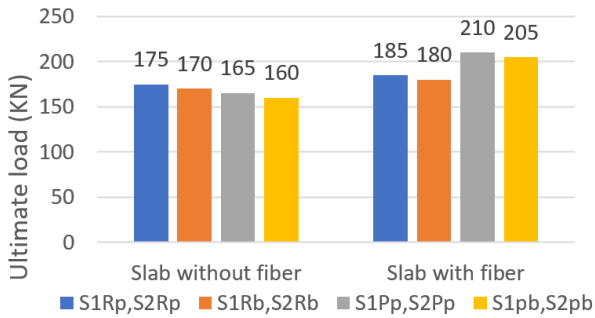


(a) The effect of distribution on Ultimate load

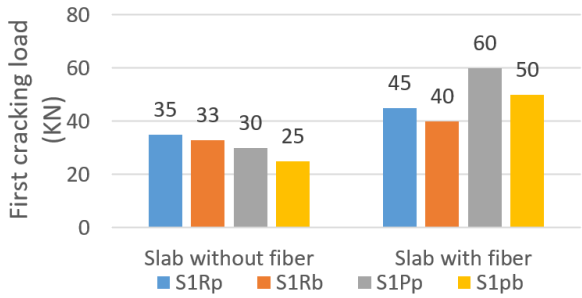


(b) The effect of distribution on first crack load

**Figure 12.** The effect of shear reinforcement distribution

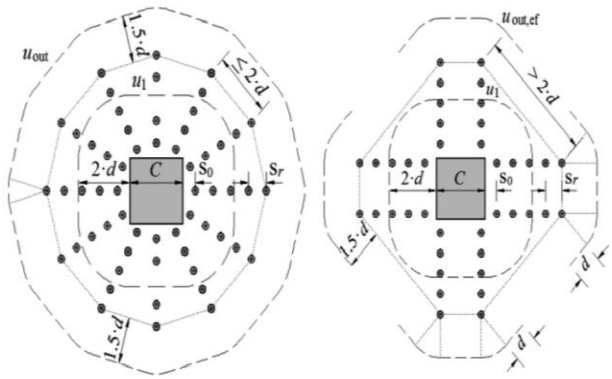


**Figure 13.** The distance between shear bar for radial and Parallel distribution [29]

The other possibility is what Cajka et al. [30] describe in Figure 14 about failure patterns with this drawing; it can be concluded which is the most effective way to distribute the shear reinforcement to resist the formation of failure in a slab with or without steel fibers. So, the parallel distribution of

shear reinforcement was the strongest in slabs with steel fiber despite the distance between them.

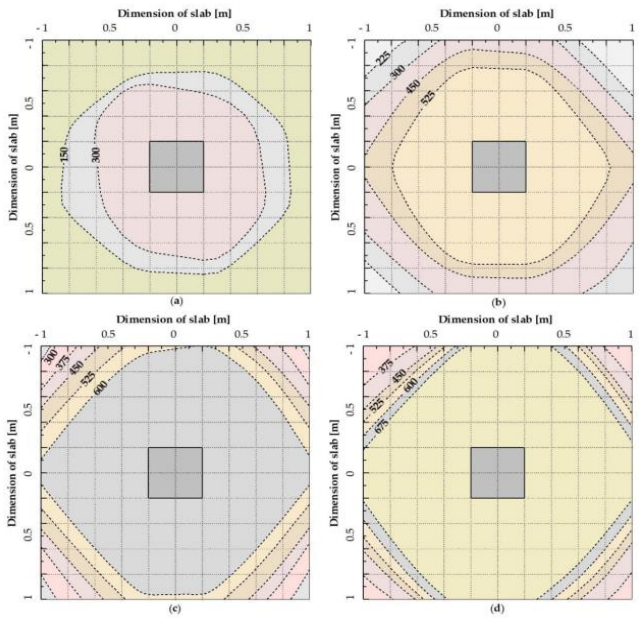


**Figure 14.** The gradual deformation Shape: a. slab without steel fiber in concrete B,c,d. Slab with steel fiber in concrete with various steel fiber ratio [30]

## 3. NUMERICAL APPLICATION

Understanding reinforced concrete slab behavior is important by carrying out full-scale experiments. In addition to experimentation, Finite Element Analysis can be used to numerically recreate the behavior, providing a valuable complement to laboratory studies. To simulate the behavior of ten slabs from linear to nonlinear response up to failure, FEM models were developed using the ABAQUS/CAE (version 2020) software. The modules in ABAQUS/CAE define the logical aspects of modelling, for example, defining geometries, materials, and generating meshes.

### 3.1 Geometry

The simulated geometry was specified to be identical to the actual dimensions of the experimental specimens. In this part, two additional models were used with stirrup shear reinforcement, one with steel fiber and the other without, see Figure 15.

The area of the stirrup bar was equal to the total area of the shear reinforcement Y-type bar. These two models were added to see how well Y-type reinforcement (plates or bars) resists the punching shear stresses.

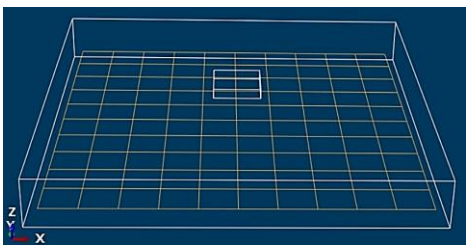

(a) Modeling of S1, S2

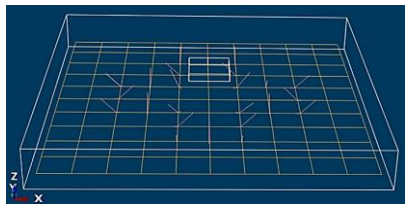

(b) Modeling of S1Pb, S2Pb

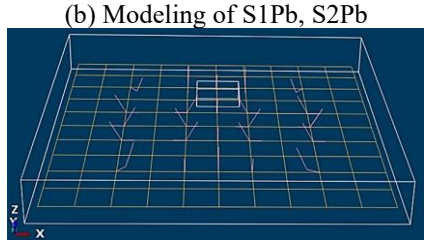

(c) Modeling of S1Rb, S2Rb

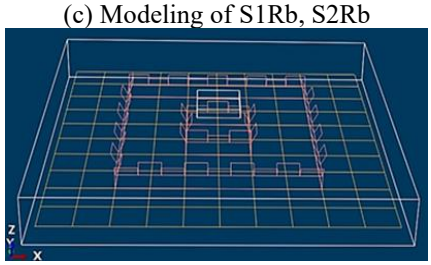

(d) Modeling of S1p, S2Pp

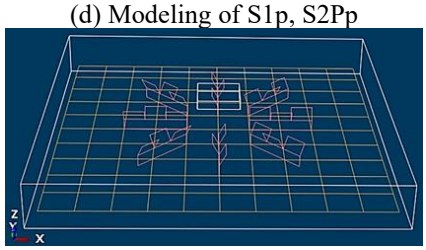

(e) Modeling of S1Rp, S2Rp

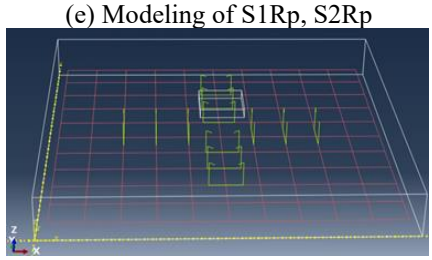

(f) Modeling of Slab with stirrups

**Figure 15.** Modeling of specimens

### 3.2 Modeling of properties

When conducting any nonlinear finite element analysis pattern, material properties are essential. Consequently, elastic and damage models can better describe concrete behavior, while plasticity models are more appropriate for steel [31].

3.2.1 Concrete properties

Concrete's behavior under different loads has been modeled using a variety of approaches such as: the (smeared crack model (SCM), brittle cracking model (BCM), and concrete damage plasticity model (CDP)). The CDP allows examining two key failure modes of concrete: tensile cracking and compression crushing. The CDP proved to be highly suited to modeling concrete behavior under various loading conditions. Due to the complexity of fibers in reinforced concrete, Abaqus software does not represent fibers in concrete, so RC with steel fiber is modeled by using the better properties (elastic and plastic behavior) of RC without steel fiber as observed in experiments [32].

In this paper concrete will be defined by elasticity and damage models.

1. Elastic: Two physical constants can be derived from simple experiments to characterize the response of a homogeneous linearly elastic material. For instance, both the Poisson ratio and Young's modulus are obtained from compression or uniaxial tension [33].

Table 3 show the Poisson ratio which was obtained by Rocco et al. [34] and by cylinder test was used to calculate the modulus of elasticity

**Table 3.** Elastic properties of concrete

| Concrete mixture | Poisson's ratio | Modulus of elasticity (MPa) |
|---|---|---|
| **Concrete without steel fiber** | 0.2 | 26437.5 |
| **Concrete with steel fiber** | 0.2 | 28117.56 |

2. Concrete damage plasticity (CDP): Three types of isotropic plasticity are used in simulating the concrete behavior in damage plasticity:

a) Plasticity can be considered an effective tool in describing ductile material behavior. It is also helpful in describing brittle behavior through finite element analysis. According to Bashar Alfarah et al. [35]. To represent the damage plasticity, 5 plastic damage factors are employed (Abaqus Documentation 2011).

•The angle of dilation (Ψ)

•The ratio of flow potential (Eccentricity)

•The ratio of "the initial compressive yield stress (fbo) to the initial uniaxial compressive yield stress (fco)"

•(K) the ratio from "the second stress invariant on the tensile meridian to the compressive meridian"

•The viscosity defines the visco-plastic normalization.

The establishment of a standard plasticity model by Alfarah et al. [35] is listed in Table 4.

**Table 4.** Plasticity properties of concrete [35]

| Dilation angle | Eccentricity | $fb_0/fc_0$ | K | Viscosity parameter |
|---|---|---|---|---|
| 13 | 0.1 | 1.16 | 0.7 | 0 |

b) Compressive behavior, In Abaqus, Uniaxial stress and inelastic hardening strain are required to model this behavior. Standard cylinder with a diameter of 150 mm, 300 mm high, used in uniaxial compression stress-strain tests; equation from Hafezolghorani et al. [36] used to calculate inelastic hardening strains based on that tests.

$$E_{in}=\epsilon-\frac{\sigma}{E} \quad \text{Hafezolghorani et al. [36]} \qquad (1)$$

where, $\sigma$ and $\epsilon$ are compressive stress and strain, respectively, they are characterized by uniaxial compression stress-strain tests, while $E$ is the modulus of elasticity. Figure 16 show the stress and inelastic strain for concrete without and with steel fiber.

c) Tensile behavior in Abaqus, the concrete tensile behavior is defined using three methods:

•Yield stress and cracking strain

•Yield stress and displacement

•Yield stress and fracture energy. According to Björnström et al. [37], the fracture energy Gf in material terms is a parameter that describes how much energy takes to open the unite area's crack to achieve stress-cracking, Gf is usually between 50 and 200 N/m for ordinary concrete, as in Bangash [38].

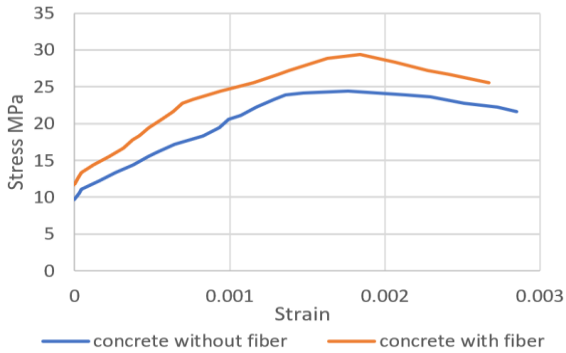


**Figure 16.** Stress and inelastic strain for concrete without and with steel fiber

In the current study, the whole three methods had tested. However, the last method gave a more realistic result. The yield stress (ft) computed by splitting, while fracture energy was calculated using CEB-FIP MC 90 [39], as in the following equation:

$$G_F=G_{fo}\left(\frac{f_{cm}}{f_{cmo}}\right)^{0.7} \quad \text{CEB-FIP MC 90 [39]} \qquad (2)$$

where, $G_F$: fracture energy [N/mm]; $G_{Fo}$: base fracture energy value which depends on the maximum size of aggregate, $d_{max}$: given in Table 5; $f_{cm}$: mean compressive strength of concrete (MPa); $f_{cmo}$: equals to 10 (MPa).

**Table 5.** $G_{Fo}$ for different maximum aggregate size [CEB-FIP MC 90 (1993)] [40]

| $D_{max}$ (mm) | 8 | 16 | 32 |
|---|---|---|---|
| $G_{Fo}$ (N/mm) | 0.025 | 0.03 | 0.058 |

The tensile behavior of reinforced concrete with and without steel fiber which is used in Abaqus is listed in the Table 6.

**Table 6.** Tensile behavior of concrete

| Tensile behavior of concrete without steel fiber | | Tensile behavior of concrete with steel fiber | |
|---|---|---|---|
| **Yield Stress (MPa)** | **Fracture energy** | **Yield Stress (MPa)** | **Fracture energy** |
| 3.04 | 0.103 | 3.21 | 0.109 |

3.2.2 Steel properties

Due to its homogeneous nature, steel properties are more easily determined by using a tension experiment, than concrete. In this study, two types of steel sections were used; plate and bar reinforcement. The elastic and plastic properties of steel reinforcement were used to define this material [31].

### 3.3 Boundary conditions and applying load

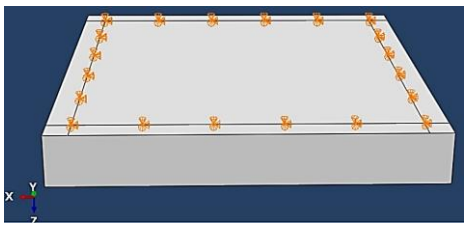

**Figure 17.** Define boundary conditions

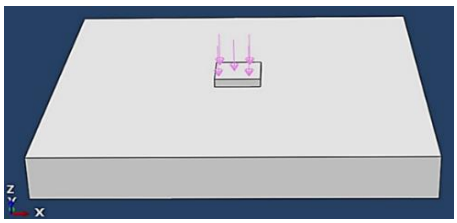

**Figure 18.** Applying load

It is necessary to apply slab boundary conditions where supports and loads exist to ensure that the model behaves in the same way as the experimental. To define fixed support in Abaqus as outlined in (section 2.3) the slabs at the support region are partitioned to define the place for fixed support, see Figure 17. As in the experiment, distribute the load on a plate with dimensions of (100 * 100 * 15) mm to model the load in Abaqus. Figure 18 shows how to apply load using a steel plate.

### 3.4 Mesh

In the initial trial, large volumes of the element are used, followed by gradual reductions until a steady state is obtained for the deflection of the specimen. Mesh sizes (50, 40, 30) mm are used and found that the best cell size is (30) mm for several reasons as; it gives the best results in terms of accuracy and realism, it is close to the result from mesh (40) mm, and analysis duration is acceptable.

### 3.5 Numerical results

3.5.1 Ultimate load and maximum deflection

Table 7 shows the ultimate loads and deflections of slabs reinforced with different concrete mixes and shear reinforcements. From that table, one can find a difference between experimental and numerical results, but that difference can be considered acceptable. For example, the largest percentage difference between a program's final load and a laboratory examination's final load was 10.2, while the deflection in the center of slabs, the largest percentage difference was 19.8.

**Table 7.** Ultimate load capacity and maximum deflection in the group for Abaqus and experimental test

| Specimens | Ultimate load (KN) | | The difference in ultimate load % | Maximum deflection (mm) | | The difference in max. Deflection % |
|---|---|---|---|---|---|---|
| | Ex. | ABAQUS | | Ex. | ABAQUS | |
| S1 | 135 | 124 | -8.1 | 6.11 | 5.74 | -6.05 |
| S1Rp | 175 | 181 | 3.4 | 4.32 | 4.29 | -0.7 |
| S1Rb | 170 | 158 | -7 | 5.89 | 5.49 | -6.7 |
| S1Pp | 165 | 161 | -2.4 | 6.69 | 6.7 | -0.15 |
| S1Pb | 150 | 165 | -1 | 7.1 | 5.75 | -19 |
| S1 Stirrup | - | 148 | - | - | 4.01 | - |
| S2 | 145 | 157 | 8.2 | 6.9 | 6.22 | -9.8 |
| S2Rp | 185 | 204 | 10.2 | 6.34 | 5.34 | -15.7 |
| S2Rb | 180 | 186 | -5 | 9.8 | 9.06 | -7.55 |
| S2Pp | 210 | 194 | -8.2 | 8.81 | 8.1 | -8 |
| S2Pb | 205 | 195 | -4.8 | 8.02 | 7.165 | -10.6 |
| S2 stirrup | - | 177 | - | - | 6.93 | - |

3.5.2 The slab behavior in Abaqus softwar

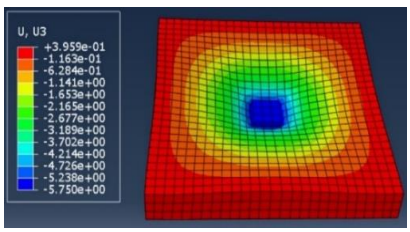


(a) Strain in slab

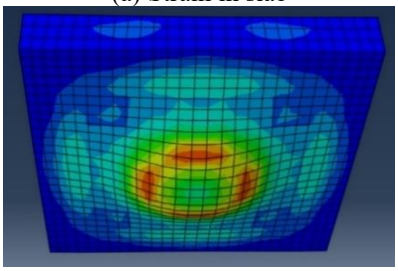

(b) Crack pattern in Abaqus

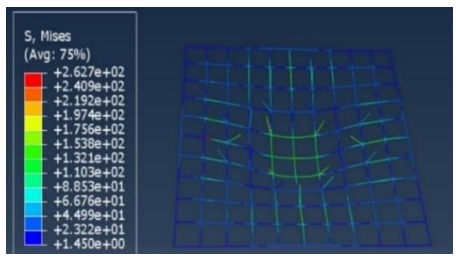


(c) Steel strain

**Figure 19.** S1Pb behavior

To validate numerical solution applications using Abaqus software used, the Slabs (S1Pb and S2Pp) have been discussed in this section.

According to Abaqus, the stress propagates from the point of applied load to the point of support in the compression path, creating a strut similar to the strut in reality. Observations of crack distributions and propagation in compression paths

somewhat agree with those from experiments. The flexural reinforcements reach higher stress than the shear reinforcements (see Figures 19 and 20).

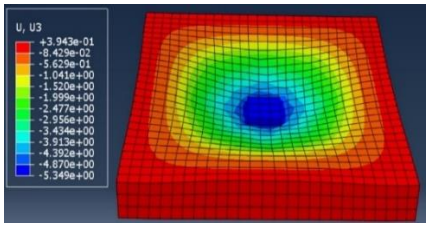


(a) Strain in slab

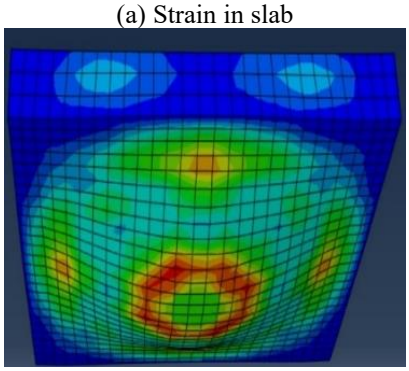

(b) Crack pattern in Abaqus

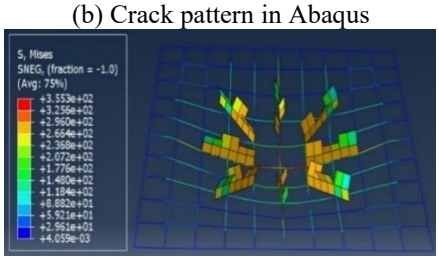


(c) Steel strain

**Figure 20.** S2Rp behavior

3.5.3 The Effect of steel fiber on ultimate load

Figure 21 shows the difference in capacity between slabs with and without fiber. Abaqus increased the load capacity of samples with steel fiber by (12.7-26.6%), but the sequence of the strongest and weakest models remained unchanged. In this case, by using properties of concrete with fiber, the loading capacity of all models was increased since the program represents concrete by its properties (elastic and plastic behavior).

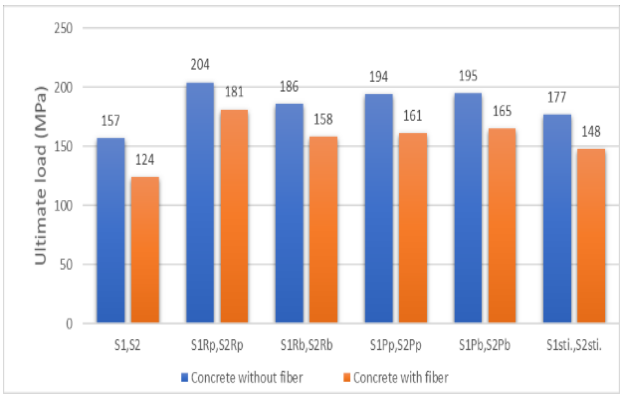


**Figure 21.** Effect of steel fiber on ultimate load in Abaqus

3.5.4 The effect of mesh size on ultimate load

Although the meshing size in the finite element approach could affect the convergence of results, this property has little impact on load-deformation charts, as in Figure 22. When the mesh size is reduced, the outputs are more accurate. However, the mesh size must not be reduced to a level that may increase the analysis duration, so the adequate mesh size was 30 mm, as observed by Ali et al. [41].

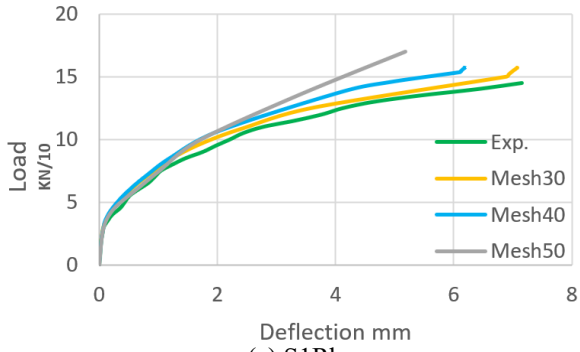


(a) S1Rb

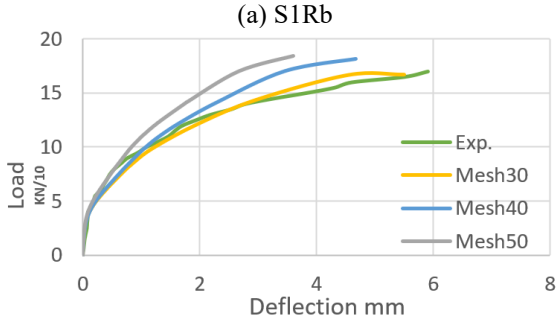


(b) S2

**Figure 22.** Mesh effect on the load-deflection curve

### 3.6 Load deflection curve

In the Abaqus program, the deflection was taken at the same location as in the experimental work. The deflection remained small until the cracking began, then the deflection increased rapidly. Figure 23 shows the load versus deflection curves gained from the numerical analysis and experimental work. It can be seen from this figure that, generally, there is an acceptable agreement between the two results, with a mild deviation in the experimental curve because the experimental environment is not ideal as in the program software.

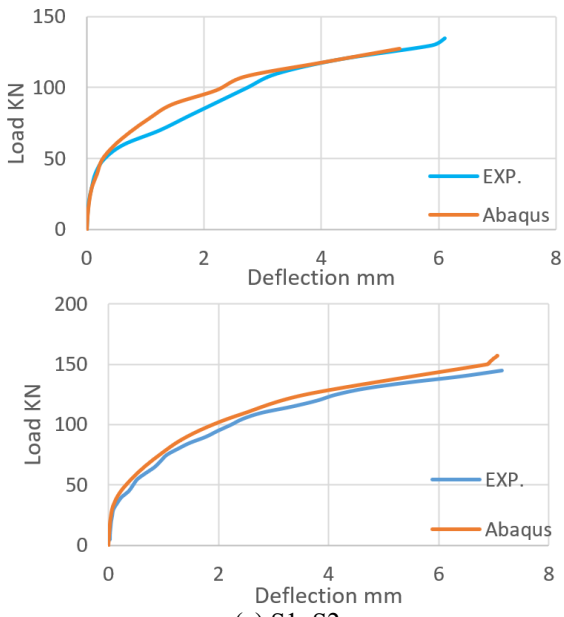


(a) S1, S2

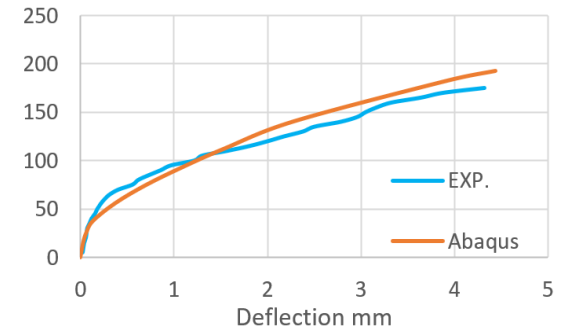


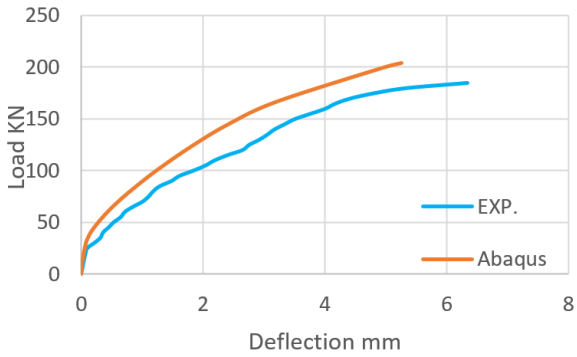


(b) S1Rp, S2Rp

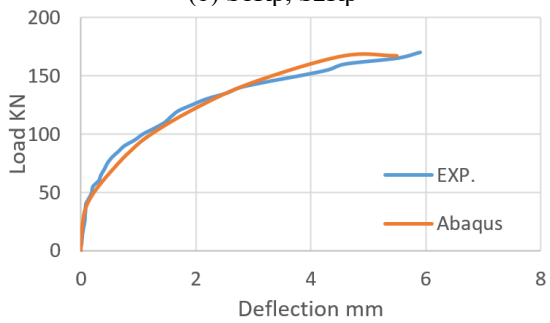


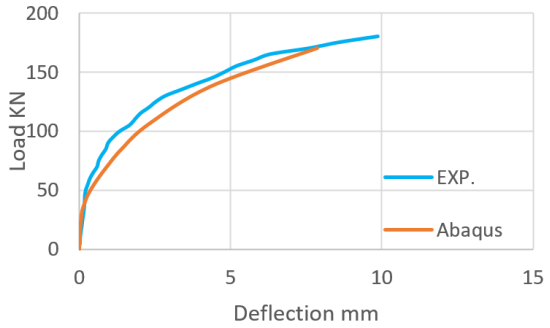


(c) S1Rb, S2Rb

**Figure 23.** Load-deflection variation for the experimental and numerical result

## 4. CONCLUSIONS

From the experimental and numerical results, the following conclusions are drawn:

1. The shear reinforcement generally provides greater strength for ultimate loads by a ratio (1.11-1.44) and the ratio of crack loads (1.25-2) compared with the control slab.

2. With steel fiber present, ultimate loads were increased about 1.07 and cracking loads were delayed about 1.5 in sample without shear reinforcement, while steel fiber increased ultimate loads by ratio (1.05-1.36) and delay cracking loads by ratio (1.5-1.7) in samples with shear reinforcement.

3. The ratio of increase in ultimate load was (1.22-1.45), when comparing samples with plate shear reinforcement to samples without shear reinforcement. The ultimate load in slab with plate shear reinforcement increased about (1.024-1.1) compared to slabs with bar shear reinforcements.

4. There was a minimal effect from shear reinforcement distribution on capacity. With steel fiber, the parallel distribution held more strength, whereas in slabs without steel fiber the parallel distribution was weaker.

5. punching shear cracks were observed at the intersection of (0.5 d-1.5 d) from the column edge to the reinforcement ends.

6. Abaqus responded as expected to the presence of the shear reinforcement because the models carried a higher load capacity by a ratio (1.12-1.46) than the model without the reinforcement.

7. Specimens with steel fiber have a greater load capacity in the range from 1.1 to 1.26 than specimens without steel fiber.

8. In comparison to slab reinforced with plate or bar shear reinforcement in Abaqus, the slab with stirrups was weaker by a ratio 1.08-1.22 compared to the slabs with plate and by a ratio (1.05-1.11) when compared to slabs with bar shear reinforcement.

## REFERENCES

[1] Ghoneim, M.A., El-Mihilmy, M.T. (2008). Design of Reinforced Concrete Structures.

[2] McCormac, J.C., Brown, R.H. (2015). Design of reinforced concrete. John Wiley & Sons.

[3] A.C. (2019). 318, Building Code Requirements for Structural Concrete (ACI 318-19): An ACI Standard; Commentary on Building Code Requirements for Structural Concrete (ACI 318R-19). American Concrete Institute.

[4] En, B. (2004). 1-2: 2004 Eurocode 2: Design of concrete structures-Part 1-2: General rules-Structural fire design. European Standards, London.

[5] Khaloo, A., Raisi, E.M., Hosseini, P., Tahsiri, H. (2014). Mechanical performance of self-compacting concrete reinforced with steel fibers. Construction and Building Materials, 51: 179-186. http://dx.doi.org/10.1016/j.conbuildmat.2013.10.054

[6] Marzouk, H.M., Hussein, A. (1990). Properties of high-strength concrete at low temperatures. ACI Materials Journal, 87(2): 167-171.

[7] Mabrouk, R.T., Bakr, A., Abdalla, H. (2017). Effect of flexural and shear reinforcement on the punching behavior of reinforced concrete flat slabs. Alexandria Engineering Journal, 56(4): 591-599. http://dx.doi.org/10.1016/j.aej.2017.05.019

[8] Saadoon, A.S., Abbas, A.M., Hussain, H.K. (2019). A review on flat slab punching shear reinforcement. Journal of University of Babylon for Engineering Sciences, 27(3): 44-58.

[9] Jang, J.I., Kang, S.M. (2019). Punching shear behavior of shear reinforced slab–column connection with varying flexural reinforcement. International Journal of Concrete Structures and Materials, 13(1): 1-14. https://doi.org/10.1186/s40069-019-0341-4

[10] Abbas, A.M., Hussain, H.K., Saadoon, A.S. (2019). Non-linear analysis to improve punching shear strength in flat slab using z-shape shear reinforcement. Muthanna Journal of Engineering and Technology, 7(1): 65-70.

http://dx.doi.org/10.52113/3/mjet/2019-7-1/65-70
[11] Sine, A., Pimentel, M., Nunes, S. (2022). Experimental investigation on punching shear behaviour of RC-(R) UHPFRC composite flat slabs without transverse reinforcement. Engineering Structures, 255: 113951. https://doi.org/10.1016/j.engstruct.2022.113951
[12] Talib, H.Y., Al-Salim, N.H.A. (2022). Improving punching shear in flat slab by replacing punching shear reinforcement by ultrahigh performance concrete. International Journal of Engineering, 35(8): 1619-1628. https://dx.doi.org/10.5829/ije.2022.35.08b.18
[13] Michels, J., Waldmann, D., Maas, S., Zürbes, A. (2012). Steel fibers as only reinforcement for flat slab construction–Experimental investigation and design. Construction and Building Materials, 26(1): 145-155. https://doi.org/10.1016/j.conbuildmat.2011.06.004
[14] Ju, H., Cheon, N.R., Lee, D.H., Oh, J.Y., Hwang, J.H., Kim, K.S. (2015). Consideration on punching shear strength of steel-fiber-reinforced concrete slabs. Advances in Mechanical Engineering, 7(5): 1687814015584251. https://doi.org/10.1177/1687814015584251
[15] Moreno, C., Ferreira, D., Bennani, A., Sarmento, A., Noverraz, M. (2015). Punching shear strengthening of flat slabs: CFRP and shear reinforcement. In Concrete–Innovation and Design, fib Symposium. Fib.
[16] Ojaimi, M.F., Altaee, M.K.E., Aljabbri, N.S. (2021). Structural behavior of two-way slabs cast with different fiber types and contents. Periodicals of Engineering and Natural Sciences (PEN), 9(3): 831-843. http://dx.doi.org/10.21533/pen.v9i3.2314
[17] Zamri, N.F., Mohamed, R.N., Awalluddin, D. (2020). The experimental studies of punching shear behaviour of reinforced concrete flat slab with the inclusion of steel fibre: Overview. In IOP Conference Series: Materials Science and Engineering, 849(1): 012087. https://doi.org/10.1088/1757-899X/849/1/012087
[18] Zamri, N.F., Mohamed, R.N., Awalluddin, D., Abdullah, R. (2022). Experimental evaluation on punching shear resistance of steel fibre reinforced self-compacting concrete flat slabs. Journal of Building Engineering, 52: 104441. https://doi.org/10.1016/j.jobe.2022.104441
[19] Kim, S.H., Heo, W.H., Woo, K.S., Jung, C.Y., Park, S.J. (2014). End-bearing resistance of Y-type perfobond rib according to rib width–height ratio. Journal of Constructional Steel Research, 103: 101-116. https://doi.org/10.1016/j.jcsr.2014.08.003
[20] Iraqi Standard No. 5: Portland Cement. Baghdad, Iraq: Central Organizationfor Standardization and Quality Control, 2019.
[21] Iraqi specifications for aggregates of natural resources used for concrete and construction. Baghdad, Iraq, 1984.
[22] bundrex. Technical Data Sheet. http://www.bundrex.com/prod-tds.html.
[23] Standard, A.S.T.M. (2011). Standard specification for steel fibers for fiber reinforced concrete. United States: ASTM International.
[24] A. A615/A615M-08b. Standard Specification for Deformed and Plain Billet-steel Bars for Concrete Reinforcement. ed: ASTM International West Conshohocken, PA, 2008.
[25] ASTM, A. (2014). Standard specification for carbon structural steel. ed: ASTM International West Conshohocken, PA, USA.
[26] Dixon, D.E., Prestrera, J.R., Burg, G.R., et al. (1991). Standard Practice for Selecting Proportions for Normal, Heavyweight, and Mass Concrete (ACI 211.1-91). Farmington Hills, MI, USA: American Concrete Institute.
[27] Musse, T.H., Liberati, E.A.P., Trautwein, L.M., Gomes, R.B., Guimarães, G.N. (2018). Punching shear in concrete reinforced flat slabs with steel fibers and shear reinforcement. Revista IBRACON de Estruturas e Materiais, 11: 1110-1121. https://doi.org/10.1590/S1983-41952018000500011
[28] Uygunoğlu, T. (2008). Investigation of microstructure and flexural behavior of steel-fiber reinforced concrete. Materials and Structures, 41(8): 1441-1449. https://doi.org/10.1617/s11527-007-9341-y
[29] Sissakis, K., Sheikh, S.A. (2007). Strengthening concrete slabs for punching shear with carbon fiber-reinforced polymer laminates. ACI Structural Journal, 104(1): 49.
[30] Cajka, R., Marcalikova, Z., Kozielova, M., Mateckova, P., Sucharda, O. (2020). Experiments on fiber concrete foundation slabs in interaction with the subsoil. Sustainability, 12(9): 3939. https://doi.org/10.3390/su12093939
[31] Taqieddin, Z.N. (2008). Elasto-plastic and damage modeling of reinforced concrete. http://dx.doi.org/10.31390/gradschool_dissertations.2616
[32] Alfaidi, H. (2021). Finite element modelling of RC beams strengthened with prestressed NSM CFRP Plate. University of Waterloo. http://hdl.handle.net/10012/16931
[33] Love, A.E.H. (2013). A treatise on the mathematical theory of elasticity. Cambridge University Press.
[34] Rocco, C., Guinea, G.V., Planas, J., Elices, M. (1995). The effect of the boundary conditions on the cylinder splitting strength. Fracture Mechanics of Concrete Structures, Wittmann FH (ed.). Aedificatio Publishers: Freiburg, Germany, pp. 75-84.
[35] Alfarah, B., López-Almansa, F., Oller, S. (2017). New methodology for calculating damage variables evolution in Plastic Damage Model for RC structures. Engineering Structures, 132: 70-86. https://doi.org/10.1016/j.engstruct.2016.11.022
[36] Hafezolghorani, M., Hejazi, F., Vaghei, R., Jaafar, M.S. B., Karimzade, K. (2017). Simplified damage plasticity model for concrete. Structural Engineering International, 27(1): 68-78. https://doi.org/10.2749/101686616X1081
[37] Björnström, J., Ekström, T., Hassanzadeh, M. (2006). Cracked concrete dams–overview and calculation methods. Report, 6: 29.
[38] Bangash, M. (2001). Manual of numerical methods in concrete. Thomas Telford London.
[39] Taerwe, L. (2008). Constitutive Modelling of High Strength/High Performance Concrete: State-of-Art Report. Fédération internationale du Béton (FIB).
[40] Taerwe, L. (2008). Constitutive Modelling of High Strength, High Performance Concrete: State-of-Art Report. Lausanne: International Federation for Structural Concrete.
[41] Ali, M., Ahmad, A., Raza, A., Iqbal, M. (2021). Experimental and finite element analysis of hybrid fiber reinforced concrete two-way slabs at ultimate limit state. SN Applied Sciences, 3(1): 1-21. https://doi.org/10.1007/s42452-020-04078-y

**NOMENCLATURE**

| | |
|---|---|
| $d_{max}$ | maximum aggregate size ,mm |
| $d$ | effective depth of the slab (mm) |
| $E_c$ | concrete modulus elasticity (MPa) |
| $f'c$ | Cylinder Compressive Strength of Concrete MPa |
| $f\,b_0$ | the initial compressive yield stress |
| $f\,c_0$ | the initial uniaxial compressive yield stress |
| $f_{cm}$ | mean compressive strength of concrete (MPa) |
| $f_{cmo}$ | compressive strength equal to 10 (MPa) |
| $f_t$ | Splitting tensile strength, (MPa) |
| $G_F$ | fracture energy [N/mm] |
| $G_{Fo}$ | base fracture energy value which depends on the maximum size of aggregate |
| $k$ | constant equal to 1.5. |
| $K$ | the ratio from "the second stress invariant on the tensile meridian to the compressive meridian" |

**Greek symbols**

| | |
|---|---|
| $\epsilon$ | concrete compressive strain, mm/mm |
| $\sigma$ | compressive stress |
| $\Psi$ | the angle of dilation |